Agrociencia

AGAVE PLANT DENSITY USING CONVOLUTIONAL NEURAL NETWORKS ON AERIAL IMAGERY

Juan **Espinoza-Hernández**[1], Gilberto de Jesús **López-Canteñs**[1*], Irineo Lorenzo **López-Cruz**[1], Eugenio **Romantchik-Kriuchkova**[1]

[1] Universidad Autónoma Chapingo. Posgrado en Ingeniería Agrícola y Uso Integral del Agua. Carretera México-Texcoco km 38.5, Chapingo, Texcoco, Estado de México, Mexico. C. P. 56227.
* Author for correspondence: glopezc@chapingo.mx

Citation: Espinoza-Hernández J, López-Canteñs G de J, López-Cruz IL, Romantchik-Kriuchkova E. 2023. Agave plant density using convolutional neural networks on aerial imagery. **Agrociencia.** doi.org/ 10.47163/agrociencia.v57i7.2970

Editor in Chief:
Dr. Fernando C. Gómez Merino

Received: February 18, 2023.
Approved: June 12, 2023.
Published in Agrociencia: October 26 2023.

ABSTRACT

Agave plants (*Agave tequilana* Weber) are an indispensable element in the tequila production chain. Traditionally, plantation monitoring has been done manually; however, having accurate information on agave inventories is crucial for planning and estimating production volume. In this context, it was proposed that deep learning algorithms can achieve high detection rates of agave plants, improving the management and control of plantations. For this purpose, YOLOv4 and YOLOv4-tiny convolutional algorithms were implemented and evaluated using high-resolution RGB aerial images captured by a remotely piloted aircraft system for the determination of agave plant density. Three flight plans were planned and carried out, with ground sampling distances of 1.10, 1.64, and 2.19 cm pixel^{-1}, respectively. The database was created, and the algorithms were evaluated for a confidence level of 0.25 and an intersection threshold over the junction of 0.50. The results showed an average mean accuracy of 0.99 for both algorithms and an F1 score of 0.95 for YOLOv4 and 0.96 for YOLOv4-tiny. Furthermore, a high detection rate (Rc) of 99 % and precision values (Pr) between 90 and 92 % were obtained. A decrease in the performance of the algorithms was observed when detecting agave tillers in images with a spatial resolution of 2.19 cm pixel^{-1}. The implemented YOLO convolutional algorithms proved to be highly robust and able to generalize agave plant characteristics at different phenological stages, allowing accurate detections. In addition, the coordinates of the detected plants were used to estimate the distance between them, with a maximum error of 20 cm.

Keywords: *Agave tequilana* Weber, YOLO algorithms, drone, precision agriculture.

INTRODUCTION

Blue agave (*Agave tequilana* Weber) is grown in the Denominación de Origen del Tequila region, which includes the Mexican states of Jalisco, Michoacán, Tamaulipas, Nayarit, and Guanajuato. It is used in the production of tequila, with the state of Jalisco accounting for more than 70 % of production (Ceja-Ramírez *et al*., 2017). Given the importance of the tequila industry, the agave field has been innovating to face several challenges, such as planting planning, agave availability, pest and disease control,

theft, and loss due to disasters. An example of this innovation is the use of remotely piloted aircraft systems (RPAS), known as drones, for surveillance work (CRT, 2016).

Because the agave plant is a strategic element in the tequila production chain, there is a need for accurate inventories to estimate yields, predict and plan production, and have control over the number of established plants (Calvario *et al*., 2020). Maintaining updated inventories provides accurate information on agave availability, vegetative stage, location, and phytosanitary status, among other aspects, allowing for better management and control. Furthermore, Mexican official standard NOM-006-SCFI-2012 establishes that all agave used in tequila production must be registered with the Consejo Regulador del Tequila A.C., and producers of *Agave tequilana* Weber must annually update their registry of plantations and properties, indicating the condition and/or status in their inventory (DOF, 2012).

Given the extensive cultivation areas, manual recording of agave plants in the fields is laborious, risky, and time-consuming. In this framework, aerial remote sensing becomes relevant through the analysis of images acquired with devices that have no physical contact with the object of interest (Lillesand *et al*., 2015). It is now possible to capture photographs using RPAS for use in object identification methods such as deep learning algorithms (Prasad *et al*., 2017).

Deep learning (DL) algorithms offer the ability to examine large amounts of data efficiently and accurately, in particular convolutional neural networks (CNNs). These networks are a type of multilayer neural network whose typical architecture is composed of single or multiple blocks of convolution and clustering layers, then one or more fully connected layers and an output layer (Sultana *et al*., 2018). In the last decade, it has been observed that the use of CNNs has been the most effective option to address object detection and classification tasks in image analysis (Prasad *et al*., 2017).

Following this approach, Ubbens *et al*. (2018) trained a CNN to count leaves in a rosette arrangement. Chen *et al.* (2017) described a method for counting apples challenged by illumination changes and occlusions of nearby foliage and fruit using two CNNs. On the other hand, Ampatzidis and Partel (2019) developed a technique applying CNNs to assess citrus phenotypic characteristics using images captured by RPAS with an accuracy of 99.9 %. These examples evidence a trend in agriculture towards the implementation of DL algorithms in image analysis, especially in terms of accuracy in plant identification and detection.

In relation to research focused on agave, Flores-Garnica *et al.* (2008) used LANDSAT 7 satellite images to identify and locate agave plantations. They used regression and classification tree methods, achieving an accuracy of 70 %. However, they faced challenges due to the variability in plant density in the plots. Furthermore, the different soil characteristics and other vegetation cover could generate confusion with agave plants. Ceja-Ramírez *et al*. (2017) determined and located the area of blue agave that presented production restrictions. They used a LANDSAT 5 satellite image and applied digital interpolation through a supervised classification process, achieving an accuracy of 73 %. Calvario *et al*. (2017) used RGB images captured by RPAS at a flight altitude of 60 m to monitor agave crops. They applied layer extraction techniques to

separate agave plants from weeds and other elements. They achieved 99 % accuracy; however, they had problems with overlap between plants.

Calvario *et al*. (2020) developed an algorithm based on mathematical morphology applied to high-resolution RGB images obtained by RPAS with the objective of counting agave plants. They observed that the accuracy of the algorithm was affected by variability in plant size in the field and lighting conditions, obtaining a range of accuracy from 83 to 98 %. Furthermore, Flores *et al.* (2021) created a database of agave plant images and performed automatic plant detection and counting using a CNN applied to RGB images captured by RPAS at an altitude of 50 m, achieving an accuracy of 96 %, but with a high computational cost.

According to the review, the trend to implement DL techniques on sets of images acquired by RPAS in agriculture is reaffirmed. However, Flores *et al*. (2021) added that YOLO convolutional algorithms can be tested in the future, as their versatility and robustness could improve processing speed. YOLO algorithms have demonstrated their efficiency in different crops; e.g., Ammar *et al*. (2021), Chowdhury *et al.* (2022), and Jintasuttisak *et al.* (2022) applied CNNs algorithms, including YOLO algorithms, for palm counting and localization; Wang *et al*. (2021) and Mota-Delfin *et al*. (2022) for counting maize plants; and Lin *et al*. (2022) detecting peanut seedlings.

Therefore, it was proposed that deep learning algorithms can achieve high detection rates of agave plants, improving the management and control of plantations. For this purpose, YOLOv4 and YOLOV4-tiny convolutional algorithms were implemented and evaluated using high-resolution RGB aerial imagery captured by a remotely piloted aircraft system for agave plant density determination.

MATERIALS AND METHODS

Experimental area

The study area is a 4.4 ha blue agave plantation located on the Guadalajara-Tepic highway km 36.2, municipality of El Arenal, Jalisco, Mexico, geographically located at coordinates 20° 47′ 35.39′′ N and 103° 42′ 4.27″ W. This study area was selected because it had agave in different phenological stages, as well as the presence of bare soil and weeds (Figure 1).

Figure 1. Characterization of the agave field (*Agave tequilana* Weber) of the experimental area, located in the municipality of El Arenal, Jalisco, Mexico. A: double row agave; B: overlap between plants; C: agave tillers; D: presence of weeds.

RPAS image acquisition and photogrammetric processing

RPAS image acquisition and photogrammetric processing was divided into two phases: field data collection and image processing.

In the first phase, a DJI Phantom 4 Pro V2.0 multirotor RPAS (SZ DJI Technology Co., Shenzhen, China) equipped with a 20 MP RGB camera with a 24 mm equivalent focal length was used. The study area was flown over on September 5, 2021, between 11:00 and 14:00 local time at three different altitudes: 40, 60, and 80 m, resulting in the following ground sampling distance (GSD) values: 1.10, 1.64, and 2.19 cm pixel^{-1}. The temperature was 27 °C, with scattered clouds and a wind speed of 5 km h^{-1}. The flight missions were planned and carried out using the DJI Pilot mobile application (SZ DJI Technology Co., Shenzhen, China), where the ISO value was set to 100, exposure value to 0, shutter to 1/400, and both lateral and frontal overlap of the images to 80 %. The images were captured from the top view (vertically), i.e., with the optical axis of the camera perpendicular to the plantation.

In the second phase, the Pix4Dmapper software (Pix4D S.A., Lausanne, Switzerland) was used to import the images and generate three orthomosaics. During this process, the internal and external calibration and orientation of the cameras were performed to reconstruct the study area.

Image labeling and database partitioning

The use of supervised learning methods involves telling the algorithm which object to find in the images. For this purpose, a database with 2403 images of size 416 x 416 pixels was created from the three orthomosaics generated. Data labeling was carried out according to the format required by YOLO, using the LabelImg tool (Tzutalin, 2015).

LabelImg was used to manually locate the position of each agave plant in each of the images, and a bounding box was drawn assigning a class, naming "Agave" to the only class, which is the one to be detected. The labeled images were randomly divided into 70 % (1683) for training, 15 % (360) for testing, and 15 % (360) for evaluation.

YOLOv4 and YOLOv4-tiny detection algorithms

YOLO uses a CNN to perform object detection in an image, and its operation is based on the division of an input image into a grid of cells. For this purpose, the algorithm employs a deep convolutional neural network to extract image features. For each cell in the grid, YOLO makes predictions over multiple bounding boxes. Each bounding box is characterized by five values: the coordinates of the box center (bx,by), the width (bw) and height (bh) of the box, and a confidence score representing the probability that the box contains an object (Figure 2A).

Likewise, YOLO uses multiple detection layers in different sizes. These layers, called "scales", are responsible for generating bounding boxes for small, medium, and large objects in the image. To avoid duplicate object detection, non-maximum suppression is applied. This technique compares the confidence scores of the bounding boxes and

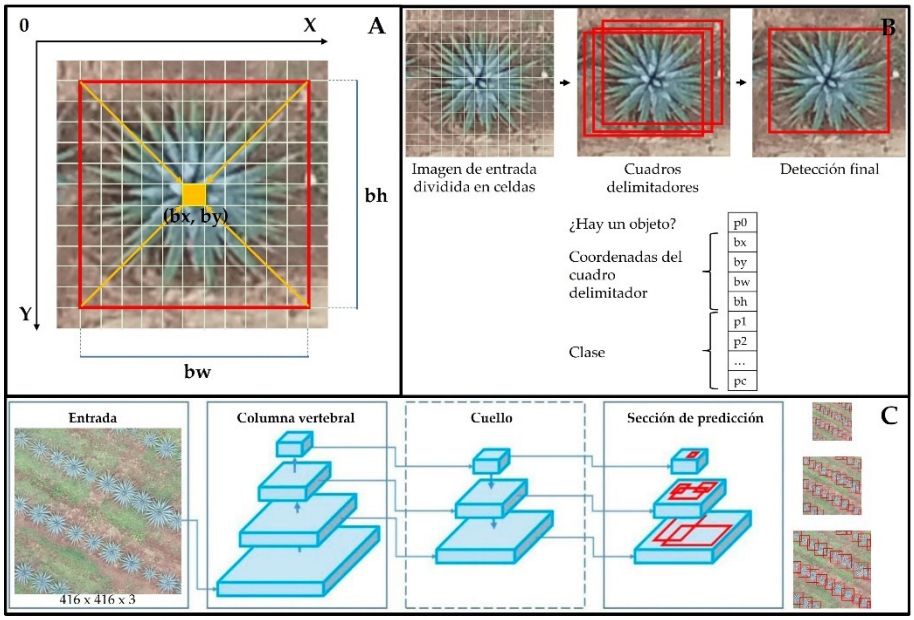

Figure 2. YOLOv4 convolutional algorithm and aspects of its operation. A: dimensions and coordinates of the YOLO bounding box; B: general flow of the YOLO algorithms to obtain the prediction vector values; C: architecture diagram of the YOLOv4 algorithm with a 416 x 416 x 3-pixel input image and three detection layers (Bochkovskiy *et al*., 2020).

suppresses boxes that have high overlap (measured by intersection over union, IoU) and lower confidence scores (Figure 2B). Finally, class labels are assigned to the selected bounding boxes, and the final object detection results are obtained. Each bounding box is associated with a specific class and is displayed with its corresponding confidence score.

The architecture of YOLOv4 is composed of four main parts: input, spine, neck, and head or prediction section (Figure 2C). As a backbone, YOLOv4 implements CSPNet + Darknet53, forming CSPDarknet53, which consists of multiple convolutional and clustering layers. This backbone is responsible for extracting feature maps to learn meaningful representations of the input image. The neck implements SPP + PANet architectures to merge features extracted by the backbone, enabling the capture of both fine details and broader features, resulting in an improved ability to detect objects of different sizes. The head is responsible for making the final predictions, consisting of detection layers that generate bounding boxes and confidence scores for the detected objects. These layers use information from multiple scales to locate and classify objects in the image.

YOLOv4 implements several techniques that improve its performance, such as Mosaic data augmentation, DropBlock regularization (Ghiasi *et al.*, 2018), CloU-loss, and Mish-activation. With Mosaic data augmentation, YOLOv4 identifies objects at a

smaller scale by combining four training images into one in certain proportions. By introducing CloU during training as a loss function, accuracy is improved. Whereas, the Mish activation function prevents the gradient (the feedback information used to adjust the parameters and weights of the network) from becoming too small and causing the neurons to stop learning or contribute minimally to the training process. Maintaining a smoother gradient ensures that the neurons receive enough information to update their weights and improve the accuracy of the model. The Mish function is mathematically defined as:

$$f(x) = x * tanh\ (ln\ (1 + exp\ (x)))$$

On the other hand, one of the differences between YOLOv4 and YOLOv4-tiny is the size and complexity of the network. This means that the tiny version has fewer convolutional layers and parameters compared to YOLOv4, resulting in a smaller model in terms of inference speed, making detections on two different scales instead of three. Furthermore, due to its lower complexity, YOLOv4-tiny may have lower detection accuracy as it is focused on fast object detection. YOLOv4 architectures were selected for their efficiency, as they are designed to be fast and offer high accuracy and detection capability.

Learning transfer

During the training of the architectures, the transfer learning approach was applied, whereby the pre-trained weights of the detection algorithms previously trained on a specific dataset were exploited. These weights were transferred and used as a starting point to train the algorithms on a new data set. This approach improves efficiency during training, in contrast to initializing the weights randomly (Wang *et al*., 2022). In this case, YOLOv4 and YOLOv4-tiny weights previously trained on the COCO database were used (Lin *et al*., 2015).

Hyperparameter setting

Hyperparameters are values that are defined prior to training and affect how a model learns and generalizes to new data (Wang *et al*., 2022). Adjusting the hyperparameters facilitates training and maximizes the number of correct detections, not only on training data but also on test data and other inputs.

Modifications were made to the YOLO source code to adapt the algorithms to the agave image dataset. The input size of the algorithm was set to the size of the images in the database, 416 x 416 x 3, where the number 3 indicates RGB images. The number of classes was set at one. The number of filters to extract features in the convolutional layers before the YOLO layers was set to 18, considering the formula: (number of classes + 5) x 3. The number of iterations was set at 6000, while other hyperparameters were kept as default (Table 1).

Table 1. Hyperparameters used for training the YOLOv4 and YOLOv4-tiny algorithms.

Algorithm	Lot	Moment	Learning rate	Decay (%)
YOLOv4	64	0.949	0.001	80 and 90
YOLOv4-tiny	64	0.9	0.00261	80 and 90

Training

The training of the algorithms was carried out using the Google Colaboratory Pro service, which provides a GPU to reduce training times when working with neural networks. The assigned GPU was a Tesla P100-PCIE-16GB.

Evaluation metrics

Precision (Pr), Recall (Rc), F1-score (F1), and mean average precision (mAP) metrics were used to evaluate the performance of the algorithms (Padilla *et al*., 2021). The Pr metric evaluates the proportion of correctly identified positive results out of the total number of results classified as positive, i.e., it measures the accuracy of an identified object being an agave plant. Recall evaluates the proportion of correctly identified positive results out of the total number of results that should have been identified as positive, i.e., it measures the ability to identify agave plants. The F1-score is the harmonic average between Pr and Rc, it is used to measure overall performance, obtaining a high value if both Pr and Rc are high. Also, mAP summarizes the average detection accuracy to a defined IoU value:

$$Pr = \frac{TP}{TP + FP}$$

$$Rc = \frac{TP}{TP + FN}$$

$$F1\ Score = 2\left(\frac{Precision * Recall}{Precision + Recall}\right)$$

where TP (true positives) are agave plants correctly identified, FP (false positives) are objects identified as agave that are not, and FN (false negatives) are unidentified agave.

Count and estimation of distance between plants

Random images were selected from the evaluation dataset, spanning different values of ground sampling distance. A manual count of the plants in the selected images was carried out to compare the results obtained by applying the YOLO algorithms.

The detections generated by the YOLO algorithms in an image captured at a height of 40 m with a GSD of 1.10 cm pixel^{-1}, which provide the coordinates of each bounding

box in the image, were used to estimate the distance between plants. The center of the bounding box (bx,by) was calculated using these coordinates, which approximates the center of an agave plant that is completely visible in the image due to its distinctive shape.

The coordinates of each plant center were used to calculate the distances in meters. The following formula was proposed for this purpose:

$$d(A, B) = \sqrt{(bx_2 - bx_1)^2 + (by_2 - by_1)^2}\left(\frac{GSD}{100}\right)$$

where A and B are the centers of the agave plants between which the distance is calculated. The values bx_1, by_1 are the coordinates of the center of plant A, and bx_2, by_2 are the coordinates of the center of plant B. The GSD is the ground sampling distance given in cm/pixel, related to the spatial resolution of the images captured by the RPAS.

Both YOLO detections and agave plant distance estimation were performed on a computer running Windows 10 (64-bit), AMD Ryzen 5 4600H processor, 512 GB solid state disk, 8 GB RAM, and NVIDIA GTX 1650 4 GB video card.

RESULTS AND DISCUSSION

Training

The loss curve during training becomes asymptotic in the range of 3 to 5 from iteration 2500 for YOLOv4, and in the range of 0.9 to 1.2 from iteration 2000 for YOLOv4-tiny, although it reaches its lowest value in the range of 0.7 to 0.9 from iteration 5000 (Figure 3A). The mAP value remains above 96 % for a confidence greater than 25 % and an IoU threshold greater than 50 % on the test data set, reaching a maximum value of 99.22 % for YOLOv4 at iteration 3660 and 99.16 % for YOLOv4-tiny at iteration 5340 (Figure 3B).

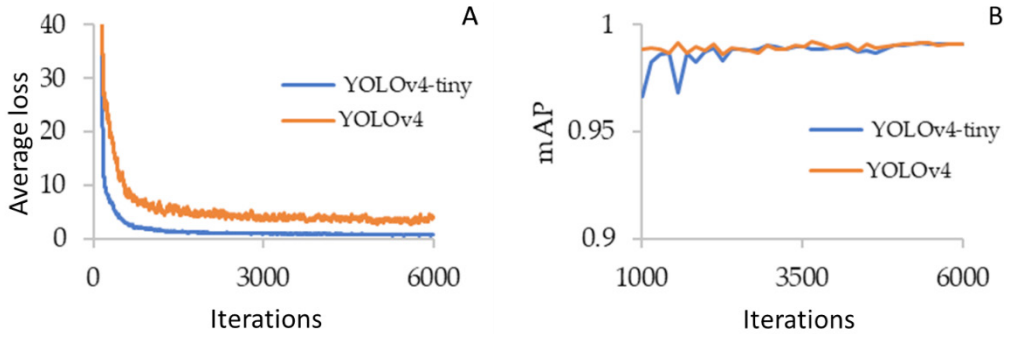

Figure 3. Curves obtained during the training of the convolutional algorithms YOLOv4 and YOLOv4-tiny for a confidence of 25 % and an IoU threshold of 50 % during 6000 iterations. A: loss-iterations curve; B: mAP-iterations curve.

Although both algorithms reached a value of 99 % in the Recall (Rc) metric, YOLOv4 had a slightly lower precision (Pr), which affected the F1 metric. Likewise, there is a difference in the training time of YOLOv4, compared to YOLOv4-tiny, due to the size of the network, its depth, and number of parameters, making the training slower in terms of computation time required (Table 2).

Table 2. Metrics obtained on the test set by the YOLOv4 and YOLOv4-tiny algorithms for a confidence of 0.25 and an IoU threshold of 0.50.

Algorithm	Training time (hours)	Pr	Rc	F1	mAP@0.50
YOLOv4	6.58	0.90	0.99	0.94	99.22
YOLOv4-tiny	0.76	0.92	0.99	0.95	99.16

Evaluation

The maximum mAP score, for a confidence greater than 25 % and an IoU threshold greater than 50 %, in the evaluation dataset was obtained by YOLOv4 with a value of 99.40 %, while YOLOv4-tiny obtained a mAP value of 99.28 %. Although both algorithms obtained 99 % in the Rc metric, it was observed that YOLOv4 obtained a lower Pr accuracy, influencing the F1 metric (Table 3).

Table 3. Metrics obtained on the evaluation dataset by the YOLOv4 and YOLOv4-tiny algorithms.

Algorithm	Pr	Rc	F1	mAP@0.50
YOLOv4	0.90	0.99	0.95	99.40
YOLOv4-tiny	0.92	0.99	0.96	99.28

Although both the F1 metric and the mAP are slightly higher in the evaluation compared to the test (Tables 2 and 3), the models do not show significant differences in percentage points in each metric, thus ensuring the absence of overfitting (Parico and Ahamed, 2021). Furthermore, the metrics obtained highlight the ability of both algorithms to effectively generalize agave plant characteristics, allowing them to make accurate predictions on new data sets. One technique that contributes to this capability is DropBlock regularization (Ghiasi *et al*., 2018). This technique consists of switching off groups of neighboring neurons in the network, which causes certain sections of the image to be temporarily hidden during the learning process. By doing this, the network is forced to learn distinct features in different regions of each image. This variation in learning helps to improve the generalization capability of the algorithm.

Another influential aspect is the random splitting of data, as in Sozzi *et al*. (2022). After reviewing the data set, it is observed that the proportion of "difficult to detect" images is lower in the evaluation set. Images with "difficult to detect" are considered to be those with agave tillers and with the highest GSD value. This means that there are fewer detection errors in the evaluation set, which slightly increases the value of the metrics.

Detection, counting, and estimation of distance between plants

The 100 % of plants detected in both algorithms were obtained for GSD values of 1.10 and 1.64 cm pixel^{-1}, corresponding to images captured at 40 and 60 m height. However, for a GSD of 2.19 cm pixel^{-1}, corresponding to images at 80 m, it was observed that YOLOv4 achieved 96.8 % detections, while YOLOv4-tiny obtained 93.6 % (Figure 4A). Both algorithms were able to detect plants even in cases of overlap between agaves and

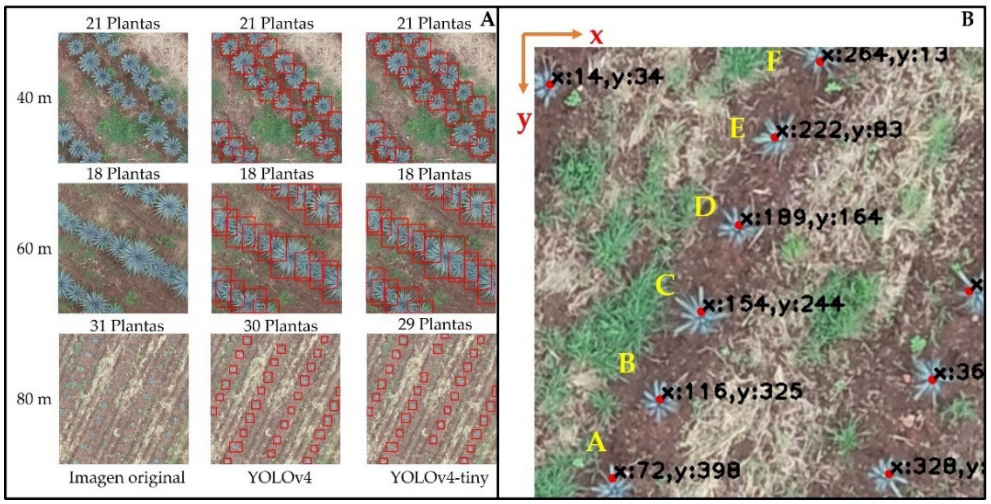

Figure 4. Detections and counts of agave plants (*Agave tequilana* Weber) A: detections and counts of agaves with YOLOv4 and YOLOv4-tiny compared to manual counting; B: centers of the detections of the bounding boxes obtained with YOLO.

presence of weeds (Calvario *et al*., 2017) at different phenological stages (Calvario *et al*., 2020). However, a decrease in performance was observed when detecting agave tillers in images with a GSD of 2.19 cm pixel^{-1}. This is attributed to the reduction in spatial resolution and the size of the plants in the images. Therefore, it is recommended to use high resolution images with a GSD of no more than 1.64 cm pixel^{-1}, especially for the accurate counting of tillers.

The estimation of distance between plants was made with the coordinates of the center of each object detected as an agave plant (Figure 4B). There is a difference between the calculated and actual distance, with plants A–B and E–F having the largest margin of error of 20 cm (Table 4).

Table 4. Comparison of the distance between Agave tequilana Weber plants calculated by applying the YOLO algorithm against the real distance between agaves.

Plants	Calculated distance (m)	Real distance (m)	Error (m)
A – B	0.94	1.14	0.20
B – C	0.98	1.10	0.12
C – D	0.96	1.09	0.13
D – E	0.96	1.13	0.17
E – F	0.90	1.10	0.20

Since the bounding boxes only take into account the visible part of the plant, there is a mismatch between the actual and predicted centroid for plants located at the edges of the image. Therefore, distance calculations can only be considered accurate for predictions of fully visible plants. Even so, an error of ± 20 cm in the calculation of the distance between plants is not significant. To be significant, the difference would have to be more than 0.90 m to be considered a missing plant, due to the planting frame of the agaves.

For example, Calvario *et al.* (2020) reported that the distance between agave plants is 1.0 to 1.20 m. Zúñiga-Estrada *et al*. (2018) mentioned a distance of 1.5 m. Due to the above, the estimated distance can be used as a reference since it has been shown that object detection and distance estimation tasks benefit each other, resulting in increased accuracy of the predicted bounding box functionality (Vajgl *et al*., 2022). Furthermore, distance estimation between objects with YOLO algorithms can be implemented in real time (Bhambani *et al*., 2020).

CONCLUSIONS

The results of this study demonstrated the versatility and robustness of the YOLOv4 and YOLOv4-tiny architectures, based on convolutional neural networks, in the detection and counting of agave plants. Furthermore, its ability to generalize agave plant characteristics was demonstrated, even in cases of overlap between agaves, different phenological stages, and the presence of weeds, overcoming the problems of overlapping found in previous research.

It was identified that the detections made by the YOLO algorithms can also be used to estimate the distance between plants. This information, combined with plant counts, is beneficial for inventorying and determining areas of vacant plantations. This methodology presents significant advantages by reducing the time required to monitor agave plantations and the risks and costs associated with manual counting.

ACKNOWLEDGMENTS

To the Consejo Nacional de Ciencia y Tecnología (CONACyT) and the Universidad Autónoma Chapingo for their support and funding for this project. To the Mexican company Vatel La Casa del Dron for providing the RPAS used in this project.

REFERENCES

Ammar A, Koubaa A, Benjdira B. 2021. Deep-learning-based automated palm tree counting and geolocation in large farms from aerial geotagged images. Agronomy 11 (8): 1458. https://doi.org/10.3390/agronomy11081458

Ampatzidis Y, Partel V. 2019. UAV-based high throughput phenotyping in citrus utilizing multispectral imaging and artificial intelligence. Remote Sensing 11 (4): 410. https://doi.org/10.3390/rs11040410

Bhambani K, Jain T, Sultanpure KA. 2020. Real-time face mask and social distancing violation detection system using YOLO. 2020 IEEE Bangalore Humanitarian Technology Conference B-HTC: 1–6. https://doi.org/10.1109/B-HTC50970.2020.9297902

Bochkovskiy A, Wang CY, Liao HYM. 2020. YOLOv4: Optimal speed and accuracy of object detection. arXiv:2004.10934 [cs.CV]. https://doi.org/10.48550/arXiv.2004.10934

Calvario G, Alarcón TE, Dalmau O, Sierra B, Hernández C. 2020. An agave counting methodology based on mathematical morphology and images acquired through unmanned aerial vehicles. Sensors 20 (21): 6247. https://doi.org/10.3390/s20216247

Calvario G, Sierra B, Alarcón TE, Hernández C, Dalmau O. 2017. A multi-disciplinary approach to remote sensing through low-cost UAVs. Sensors 17 (6): 1411. https://doi.org/10.3390/s17061411

Ceja-Ramírez R, González-Eguiarte DR, Ruiz-Corral JA, Rendón-Salcido LA, Flores-Garnica JG. 2017. Detección de restricciones en la producción de agave azul (*Agave tequilana* Weber var. Azul) mediante percepción remota. Terra Latinoamericana 35 (3): 259–268. https://doi.org/10.28940/terra.v35i3.252

Chen SW, Shivakumar SS, Dcunha S, Das J, Okon E, Qu C, Taylor CJ, Kumar V. 2017. Counting apples and oranges with deep learning: a data-driven approach. IEEE Robotics and Automation Letters 2 (2): 781–788. https://doi.org/10.1109/LRA.2017.2651944

Chowdhury PN, Shivakumara P, Nandanwar L, Samiron F, Pal U, Lu T. 2022. Oil palm tree counting in drone images. Pattern Recognition Letters 153: 1–9. https://doi.org/10.1016/j.patrec.2021.11.016

CRT (Consejo Regulador del Tequila). 2016. Agave y tequila un binomio de éxito. Consejo Regulador del Tequila A.C. Zapopan, México. https://www.crt.org.mx/images/Documentos/Libro/AGAVE_TEQUILA_UN_BINOMIO_DE_EXITO.pdf (Retrieved: July 2021).

DOF (Diario Oficial de la Federación). 2012. NORMA Oficial Mexicana NOM-006-SCFI-2012, Bebidas alcohólicas-Tequila-Especificaciones. Secretaría de Gobernación. Ciudad de México, México. http://www.dof.gob.mx/nota_detalle.php?codigo=5282165&fecha=13/12/2012 (Retrieved: July 2021).

Flores D, González-Hernández I, Lozano R, Vázquez-Nicolas JM, Hernández-Toral JL. 2021. Automated agave detection and counting using a convolutional neural network and unmanned aerial systems. Drones 5 (1): 4. https://doi.org/10.3390/drones5010004

Flores-Garnica JG, Reich R, Talavera-Zúñiga E, Aguirre-Bravo C. 2008. Using remote sensing to support different approaches to identify agave (*Agave tequilana* Weber) crops. The International Archives of the Photogrammetry, Remote Sensing and Spatial Information Sciences 37 (4): 941–944.

Ghiasi G, Lin TY, Le QV. 2018. DropBlock: A regularization method for convolutional networks. arxiv:1810.12890 [cs]. https://doi.org/10.48550/arXiv.1810.12890

Jintasuttisak T, Edirisinghe E, Elbattay A. 2022. Deep neural network based date palm tree detection in drone imagery. Computers and Electronics in Agriculture 192: 106560. https://doi.org/10.1016/j.compag.2021.106560

Lillesand T, Kiefer RW, Chipman J. 2015. Remote sensing and image interpretation (Seventh edition). John Wiley & Sons: New York, NY, USA. 768 p.

Lin TY, Maire M, Belongie S, Bourdev L, Girshick R, Hays J, Perona P, Ramanan D, Zitnick CL, Dollár P. 2015. Microsoft COCO: Common Objects in Context. arXiv:1405.0312 [cs]. https://doi.org/10.48550/arXiv.1405.0312

Lin Y, Chen T, Liu S, Cai Y, Shi H, Zheng D, Lan Y, Yue X, Zhang L. 2022. Quick and accurate monitoring peanut seedlings emergence rate through UAV video and deep learning. Computers and Electronics in Agriculture 197: 106938. https://doi.org/10.1016/j.compag.2022.106938

Mota-Delfin C, López-Canteñs G de J, López-Cruz IL, Romantchik-Kriuchkova E, Olguín-Rojas JC. 2022. Detection and counting of corn plants in the presence of weeds with convolutional neural networks. Remote Sensing 14 (19): 4892. https://doi.org/10.3390/rs14194892

Padilla R, Passos WL, Dias TLB, Netto SL, da Silva EAB. 2021. A comparative analysis of object detection metrics with a companion open-source toolkit. Electronics 10 (3): 279. https://doi.org/10.3390/electronics10030279

Parico AIB, Ahamed T. 2021. Real time pear fruit detection and counting using YOLOv4 models and deep SORT. Sensors 21 (14): 4803. https://doi.org/10.3390/s21144803

Prasad MVD, Lakshmamma BJ, Chandana AH, Komali K, Manoja M, Rajesh-Kumar P, Raghava-Prasad C, Inthiyaz S, Sasi-Kiran P. 2017. An efficient classification of flower images with convolutional neural networks. International Journal of Engineering and Technology 7 (1.1): 384. https://doi.org/10.14419/ijet.v7i1.1.9857

Sozzi M, Cantalamessa S, Cogato A, Kayad A, Marinello F. 2022. automatic bunch detection in white grape varieties using YOLOv3, YOLOv4, and YOLOv5 deep learning algorithms. Agronomy 12 (2): 319. https://doi.org/10.3390/agronomy12020319

Sultana F, Sufian A, Dutta P. 2018. Advancements in image classification using convolutional neural network. 2018 Fourth International Conference on Research in Computational Intelligence and Communication Networks (ICRCICN): 122–129. https://doi.org/10.1109/ICRCICN.2018.8718718

Tzutalin. 2015. LabelImg. https://github.com/tzutalin/labelImg (Retrieved: July 2021).

Ubbens J, Cieslak M, Prusinkiewicz P, Stavness I. 2018. The use of plant models in deep learning: An application to leaf counting in rosette plants. Plant Methods 14 (1): 6. https://doi.org/10.1186/s13007-018-0273-z

Vajgl M, Hurtik P, Nejezchleba T. 2022. Dist-YOLO: fast object detection with distance estimation. Applied Sciences 12 (3): 1354. https://doi.org/10.3390/app12031354

Wang L, Xiang L, Tang L, Jiang H. 2021. A convolutional neural network-based method for corn stand counting in the field. Sensors 21 (2): 507. https://doi.org/10.3390/s21020507

Wang Z, Jin L, Wang S, Xu H. 2022. Apple stem/calyx real-time recognition using YOLO-v5 algorithm for fruit automatic loading system. Postharvest Biology and Technology 185: 111808. https://doi.org/10.1016/j.postharvbio.2021.111808

Zúñiga-Estrada L, Rosales Robles E, Yáñez-Morales MJ, Jacques-Hernández C. 2018. Características y productividad de una planta MAC, *Agave tequilana* desarrollada con fertigación en Tamaulipas, México. Revista Mexicana de Ciencias Agrícolas 9 (3): 553–564. https://doi.org/10.29312/remexca.v9i3.1214